# Quantum theory of femtosecond optomagnetic effects for rare-earth ions in DyFeO$_3$

A. I. Popov,[1,2] K. A. Zvezdin,[1,3] Z. V. Gareeva ®,[4,5] A. V. Kimel,[6] and A. K. Zvezdin[3,7]

[1]*Moscow Institute of Physics and Technology (State University), 141700 Dolgoprudny, Russia*
[2]*National Research University of Electronic Technology, 124498 Zelenograd, Moscow, Russia*
[3]*Prokhorov General Physics Institute of the Russian Academy of Sciences, 119991 Moscow, Russia*
[4]*Institute of Molecule and Crystal Physics, Subdivision of the Ufa Federal Research Center of the Russian Academy of Sciences, 450075 Ufa, Russia*
[5]*Bashkir State University, 450000 Ufa, Russia*
[6]*Institute for Molecules and Materials, Radboud University Nijmegen, Toernooiveld 1, 6525 ED Nijmegen, The Netherlands*
[7]*P. N. Lebedev Physical Institute of the Russian Academy of Sciences, 119991 Moscow, Russia*

Our theoretical analysis shows that a femtosecond laser pulse can efficiently launch magnetization dynamics of Dy$^{3+}$ ions in DyFeO$_3$ and DyAlO$_3$. Excitation of electrons from the ground state to the low-lying electronic level of Dy$^{3+}$ ions by circularly or linearly polarized light can be seen as a result of an effective magnetic field acting on the magnetic moments of the rare-earth ions. It is shown that the launched magnetization dynamics can be expressed as a combination of coherent oscillations of mutually parallel and mutually antiparallel magnetic moments of Dy$^{3+}$ ions, respectively. While the antiparallel magnetic moments lie in the plane perpendicular to the wave vector of light in the medium $\boldsymbol{k}$, the parallel magnetic moments are aligned along $\boldsymbol{k}$. The magnetization dynamics depend strongly on the duration and the shape of the pumping laser pulse, as well as on the anisotropy in properties of the rare-earth ion.

## I. INTRODUCTION

The ability to control and switch magnetization between two stable bit states is the main principle of modern data storage technology. Due to many new ideas, originating from fundamental research during the past 50 years, this technology has developed in a breathtaking fashion, and today it faces yet another challenge. Ever increasing demands for faster and more energy-efficient data storage stimulate fundamental studies of the ways to control the magnetic state of media with the lowest possible production of heat and at the fastest possible timescale.

Femtosecond laser pulse is the shortest stimulus in contemporary experimental physics of condensed matter. The desire to understand the response of magnets to such a stimulus has led to the seminal discovery [1] of ultrafast demagnetization of Ni, and to the new field of ultrafast magnetism. The problem of conservation and transfer of angular momentum has become the central issue of this research field [2–6]. It is remarkable that although most of the theories in ultrafast magnetism take into account only the magnetism of spins, the most intriguing experimental results have been obtained on compounds containing rare-earth ions, for which the spin-orbit interaction is so strong that spin and orbital moments are not mutually independent, and orbitals contribute substantially to the net magnetization [7–18].

The goal of this work is to explore magnetization dynamics triggered by femtosecond laser pulses in rare-earth ions with strongly coupled spin and orbital degrees of freedom. To explore the mechanisms of ultrafast magnetization dynamics, research is frequently focused on rare-earth orthoferrites [7,9,14,19,20]. Due to the inherently fast spin dynamics, this class of materials serves as an excellent playground to investigate this phenomenon. Here, we consider dysprosium orthoferrite DyFeO$_3$ and dysprosium perovskite DyAlO$_3$. These compounds crystallize in an orthorhombic structure with the space group *Pnma*, so that the local environment of a single Dy$^{3+}$ ion has octahedral symmetry. Magnetic moment Fe$^{3+}$ and Dy$^{3+}$ ions get ordered at different temperatures. The Néel temperature $T_N$ for spins of Fe$^{3+}$ ions is 600–700 K, while the Néel temperature $T_N$ of Dy$^{3+}$ ions is around 10 K. To exclude any interactions between magnetic moments of Fe$^{3+}$ and Dy$^{3+}$, we also consider DyAlO$_3$. The Dy$^{3+}$ ion in DyFeO$_3$ has a well-studied electronic structure and well-defined low-lying states [21–23]. The absorption spectrum of the Dy$^{3+}$ ion reveals excited electronic states very close to the photon energy of Ti-sapphire lasers with the central wavelength $\lambda = 0.8\ \mu$m.

In Refs. [7,24,25], femtosecond laser-induced magnetization dynamics in DyFeO$_3$ has been described in terms of Raman scattering of light by spins of Fe$^{3+}$ sublattices. In contrast to [7,24,25], in this paper we explore the spin and orbital dynamics of Dy$^{3+}$ ions. Aiming to understand magnetization dynamics after a laser pulse, we calculate dynamical magnetic configurations on timescales significantly exceeding the pump-pulse duration of 100 fs.

Our findings show that an ultrashort laser pulse triggers a complex coherent dynamics of magnetic moments of $Dy^{3+}$ ions in $DyFeO_3$ and $DyAlO_3$. The dynamics depends strongly on the duration and shape of the pump pulse. The laser-induced magnetization oscillates at a frequency $\nu = E_1/2\pi\hbar = 1.58 \times 10^{12}$ Hz, which is much higher than the spin resonance frequencies of the $Fe^{3+}$ ions in $DyFeO_3$. Here $E_1 = 52.5$ cm$^{-1}$ is the energy of the electronic transition from the ground state to the low-lying electronic level of the $Dy^{3+}$ ion in the crystal field. Due to the mismatch between the frequencies of magnetization dynamics of $Fe^{3+}$ and $Dy^{3+}$ ions, any influence of the $Fe^{3+}$ spin dynamics on the magnetization dynamics of $Dy^{3+}$ and optically induced spin transfer (OIST), in particular [2,3,5,6], can be neglected.

An unexpected result of our study is the emergence of a dynamic inhomogeneous antiferromagnetic structure in the rare-earth magnet (for example, C-type structure). Usually such structures arise at low temperatures ($T \approx 4$ K) [26,27] due to "$f$-$f$" interactions between rare-earth ions. However, contrary to the previous reports in Refs. [26,27], the dynamic structure, induced by electromagnetic radiation, as reported in this work, can exist at much higher temperatures.

## II. NONSTATIONARY THEORY FOR ULTRASHORT ELECTROMAGNETIC PULSES

To consider the interaction between light and magnetic moments, we generalize the quantum-mechanical approach suggested by Pershan *et al.* [28,29] in the case of ultrashort femto- and attosecond laser pulses. We take the Hamiltonian that describes the interaction of a monochromatic electromagnetic wave with the $Dy^{3+}$ ion in $DyFeO_3$,

$$\hat{H} = \hat{H}_0 + \hat{V}, \tag{1}$$

where $\hat{H}_0$ is the crystal-field (CF) Hamiltonian for an unperturbed $Dy^{3+}$ ion, and $\hat{V}$ is the potential describing light-induced perturbation of the ground state.

Note that the CF Hamiltonian of orthoferrites consists of two parts—$\hat{H}_{CF}^{even}$ and $\hat{H}_{CF}^{odd}$—containing even and odd terms of irreducible tensor operators, respectively. The even contribution $\hat{H}_{CF}^{even}$ is accounted for in $\hat{H}_0$, while the odd contribution $\hat{H}_{CF}^{odd}$, arising due to the low symmetry of the ion environment, is accounted for in the perturbation Hamiltonian [30]

$$\hat{V} = -\boldsymbol{E}\boldsymbol{d} + \hat{H}_{CF}^{odd}, \tag{2}$$

where $\boldsymbol{d} = -e\sum_n \boldsymbol{r}_n$ is the operator of the dipole moment of the rare-earth ion with $n$ electrons in the $4f$ shell, and $\boldsymbol{E}$ is the electric field of the light wave.

The combined effect of the CF and the electric field of an electromagnetic wave on rare-earth ions is accounted for in the effective potential $\hat{V}_{eff} = -\boldsymbol{E}\hat{\boldsymbol{D}}_{eff}$, where $\boldsymbol{D}_{eff}$ are the operators of the effective dipole moment calculated in Appendix A.

We emphasize that the main role of $\hat{H}_{CF}^{odd}$ in our case is a renormalization of the electric dipole coupling between light and matter. To explore the evolution of the spin subsystem in time, we employ the Schrödinger equation $i\hbar\partial\psi_g/\partial t = \hat{H}\psi_g$ with the wave function $\psi$ taken in terms of the eigenfunctions $\phi_g$ of the Hamiltonian $\hat{H}_0$, where $E_k$ are the energies of

electronic transitions in $Dy^{3+}$,

$$\psi_g(t) = \sum_{lg} a_{lg}(t) \exp(-i\omega_l t)\phi_l$$

$$= \phi_g \exp(-i\omega_l t) + \psi_{1g}(t) + \psi_{2g}(t) + \cdots, \tag{3}$$

where $\phi_g$ does not depend on $t$,

$$\psi_{1g}(t) = \sum_l a_{lg}^{(1)}(t) \exp(-i\omega_l t)\phi_l,$$

$$\psi_{2g}(t) = \sum_f a_{fg}^{(2)}(t) \exp(-i\omega_f t)\phi_f, \tag{4}$$

and

$$a_{lg}^{(1)}(t) = \frac{1}{i\hbar} \int_{-\infty}^{t} \exp(i\omega_{lg}t')V_{lg}(t')dt',$$

$$a_{fg}^{(2)}(t) = \frac{1}{(i\hbar)^2} \sum_l \int_{-\infty}^{t} V_{fl}(t') \exp(i\omega_{fl}t')$$

$$\times \int_{-\infty}^{t'} V_{lg}(t'') \exp(i\omega_{lg}t'')dt''dt'. \tag{5}$$

In Eqs. (3)–(5), $\omega_l = E_l/\hbar$, $\omega_{lg} = (E_l - E_g)/\hbar$, and $V_{lg}(t) = \langle\phi_l|\hat{V}(t)|\phi_g\rangle$. The summation in $a_{fg}^{(2)}(t)$ is conducted on the intermediate states $\phi_l$ which connect the initial ($\phi_g$) and the final ($\phi_l$) states of the ion.

Generally, the perturbation Hamiltonian reads

$$\hat{V}(t) = \hat{v}\exp(i\omega t) + \hat{v}^*\exp(-i\omega t), \tag{6}$$

where $\hat{v}$ is determined by Eq. (2). In cases when the amplitude of light wave field $\hat{v}$ does not noticeably change in time, we get

$$a_{lg}^{(1)}(t) \approx -\frac{1}{\hbar}\left(v_{lg}\frac{e^{i(\omega_{lg}+\omega)t}}{\omega_{lg}+\omega} + v_{lg}^*\frac{e^{i(\omega_{lg}-\omega)t}}{\omega_{lg}-\omega}\right),$$

$$a_{fg}^{(2)}(t) \approx \frac{1}{\hbar^2}\sum_l\left(\frac{v_{fl}^*v_{lg}}{\omega_{lg}+\omega} + \frac{v_{fl}v_{lg}^*}{\omega_{lg}-\omega}\right)\frac{e^{i\omega_{fg}t}}{\omega_{fg}}. \tag{7}$$

Furthermore, we consider pulse excitations determined by Eq. (6), whose amplitude $\hat{v}$ depends on time as a Gaussian,

$$\hat{v}(t) = \hat{v}_0 e^{-t^2/\tau^2},$$

$$\hat{v}_0 = -E_0\hat{\boldsymbol{D}}_{eff}, \tag{8}$$

where $E_0$ is the peak value of the electric field in the pulse, and $\tau$ is the pulse duration.

In the most general case of elliptically polarized light, the amplitude $E_0$ is a complex number, effective dipole moment operators $\boldsymbol{D}_{eff}$ are the real operators, and the amplitudes $a_{lg}^{(1)}(t)$ and $a_{fg}^{(2)}(t)$ have a more complex form compared to the expressions given by Eq. (7).

Using the analogy with stimulated Raman scattering of light by magnons, we consider a Raman process that allows an excitation of low-lying states of $Dy^{3+}$ ions by photons of a much higher energy. In this case, the second and third terms in Eq. (3) [see (4)] are sufficient to account for the low-frequency excitations.

We explore laser-induced transitions between electronic states in the $Dy^{3+}$ ion. The ground state of the $Dy^{3+}$ ion is

$^6H_{15/2}$ being an Ising doublet with the orbital moment $L = 5$, the spin moment $S = 5/2$, and the total magnetic moment $J = 15/2$. The crystal field splits multiplet $^6H_{15/2}$ into doublets with the energies $E_0 = 0$, $E_1 \approx 52$ cm$^{-1}$, $E_2 \approx 147$ cm$^{-1}$, $E_3 \approx 225$ cm$^{-1}$, etc. [21]. The ground Ising doublet with the energy $E_0 = 0$ is described by the wave function $|\pm 15/2\rangle$; the first excited doublet with the energy $E_1 \approx 52$ cm$^{-1}$ is the Ising doublet described by the wave functions $|\pm 13/2\rangle$ (Appendix C). Furthermore, we consider the transitions between these states, since the next doublets have much higher energy and have a negligible impact on the laser-induced dynamics.

The photon energy of laser pulses commonly used in ultrafast time-resolved experiments is around 1.5 eV (the wavelength is 800 nm) [8,19]. It is quite close to the difference between the energies of multiplets $^6H_{15/2}$ and $^6F_{5/2}$ of Dy$^{3+}$ ions ($\approx 12 \times 10^3$ cm$^{-1}$) [31]. An entanglement between the ground $4f^N$ ($N$ is the number of electrons in the electronic shell) and the excited $4f^{N-1}5d$, $4f^{N-1}5g$ configurations of the Dy$^{3+}$ ion, which arises due to the low-symmetry CF, allows electric-dipole transitions $^6H_{15/2} \rightarrow ^6F_{5/2}$. Note that without the entanglement, such a transition must be forbidden by parity and quantum number $J$. Hence $^6F_{5/2}$ is practically an intermediate state in the analysis of the laser-induced magnetization dynamics of Dy$^{3+}$ ions in DyFeO$_3$.

It can be shown (see Appendix C) that the wave function $\psi_g$ acquires the form

$$|\pm g\rangle = |\pm 15/2\rangle + Q_\pm^{(2)}(E, t)|\pm 13/2\rangle. \quad (9)$$

For a case close to the resonance $\omega \approx \omega_0$, one finds

$$Q_\pm^{(2)}(E, t) = \sqrt{\pi} q_\pm^{(2)}(EE^*)\left(\frac{\tau}{T}\right)^2 f_{\tau -}(t), \quad (10)$$

where $T = 2\pi/\omega$,

$$q_\pm^{(2)}(EE^*) = \pm(q_1 E_\mp E_z^* - q_2 E_z E_\pm^*) - i(q_3 E_\mp E_\pm^* + q_4|E_z|^2),$$
$$E_\pm = E_x \pm iE_y,$$
$$E_\pm^* = E_x^* \pm iE_y^*, \quad (11)$$

$$q_1 = \left(\frac{T}{8\hbar}\right)^2 R\big(C_{5/2\,5/2\,6\,4}^{15/2\,13/2} C_{5/2\,5/2\,6\,5}^{15/2\,15/2} K_4 K_5'$$
$$- K_5 K_6' C_{5/2\,3/2\,6\,5}^{15/2\,13/2} C_{5/2\,3/2\,6\,6}^{15/2\,15/2}\big),$$
$$q_2 = q_1(K \rightleftharpoons K'),$$
$$q_3 = q_1(K' \rightarrow K),$$
$$q_4 = q_1(K \rightarrow K'), \quad (12)$$

$$f_{\tau -} = \exp(-i\omega_1 t) F_{-}(t), \quad (13)$$

$$F_{\tau -}(t) = \frac{1}{\tau}\int_{-\infty}^t \phi_-(t')dt', \quad (14)$$

$$\phi_-(t) = \exp\left(-\frac{2t^2}{\tau^2} + i\omega_1 t\right)\exp(Z_-^2(t))\mathrm{erfc}(Z_-(t)), \quad (15)$$

$$Z_-(t) = \frac{i}{2}\tau(\omega_0 - \omega) - \frac{t}{\tau}. \quad (16)$$

Here we account for $|\phi_+(t)| \ll |\phi_-(t)|$ (see also Appendixes B and C).

$Q_\pm^{(2)}(E, t)$ defines the quantum torque generated by the laser pulse. The torque changes the direction of the magnetic moment of the Dy$^{3+}$ ion as a result of the electronic transition from the ground state $|15/2\rangle$ to the excited state $|13/2\rangle$. We therefore conclude that the laser pulse generates a magnetic torque, which results in a rotation of the magnetic moment of the Dy$^{3+}$ ion.

Let us explore the transformation of the magnetic structure under the action of linear and circular polarization laser pulse. We assume that the light propagates along the "$b$" axis of the crystal. The components of the vector $\boldsymbol{E}$ in the coordinate system composed of the crystallographic axes are

$$E_x^{(k)} = E_c(c\boldsymbol{e}_k^x), \; E_y^{(k)} = E_a(a\boldsymbol{e}_k^y), \; E_z^{(k)} = E_a(a\boldsymbol{e}_k^z), \quad (17)$$

where $\boldsymbol{e}_k^\alpha$, $k = 1, \ldots, 4$ are determined as

$$\boldsymbol{e}_k^x = (0, 0, (-1)^k), \; \boldsymbol{e}_{1,2}^y = (-\sin(\alpha), \pm\cos(\alpha), 0),$$
$$\boldsymbol{e}_k^x = (\cos(\alpha), \pm\sin(\alpha), 0), \; \boldsymbol{e}_{3(4)}^y = -\boldsymbol{e}_{1(2)}^y,$$
$$\boldsymbol{e}_{3(4)}^z = -\boldsymbol{e}_{1(2)}^z, \quad (18)$$

where $E_{a,c}$ are the projections of vector $\boldsymbol{E}$ on the axes $a$ and $c$.

In the $\Gamma_4$ phase, the magnetic field $\boldsymbol{H}\|\boldsymbol{c}$ induces a magnetic moments of Dy$^{3+}$ ions aligned along the $c$-axis. At low temperatures $T_M < T < E_1/k_B = 78$ K, the corresponding magnetization is $M_c^0 = 15(\mu_B g_J)^2 H_c/\hbar\omega_1$. If the field is generated by a laser pulse, it would induces a transient magnetization of Dy$^{3+}$ ions,

$$M_\alpha = \langle g_+|\mu_\alpha|g_+\rangle + \langle g_-|\mu_\alpha|g_-\rangle, \quad (19)$$

where $\mu_\alpha = -g\mu_B J_\alpha$ is the operator of the magnetic moment component, $g = 4/3$ is the Landé factor for the Dy$^{3+}$ ion, and $\pm g\rangle = |\pm 15/2\rangle + Q_\pm^{(2)}(E, t)|\pm 13/2\rangle$. Below we consider the case of incident light waves with linear and circular polarizations.

## III. ULTRASHORT INVERSE QUANTUM COTTON-MOUTON EFFECT

Consider a linearly polarized wave (i.e., the amplitudes $E_\alpha$ are real). We keep only the principal components containing $f_{\tau -}(t)$. It can be shown [see Eq. (C3)] that

$$M_a^{(k)} = \pm\mu_{\mathrm{eff}} E_c E_a(q_1 - q_2)\sin(2\alpha)A_\tau(t)\left(\frac{\tau}{T}\right)^2$$
$$\times \sin[\omega_1 t - \beta_\tau(t)],$$

$$M_b^{(k)} = 2\mu_{\mathrm{eff}} E_c E_a(q_1 - q_2)\cos^2\alpha A_\tau(t)\left(\frac{\tau}{T}\right)^2$$
$$\times \sin[\omega_1 t - \beta_\tau(t)],$$

$$M_c^{(k)} = \pm\mu_{\mathrm{eff}}\bigg[q_3 E_c^2 + E_a^2\bigg(q_3\sin^2\alpha + q_4\cos^2\alpha$$
$$- \frac{q_1 + q_2}{2}\sin(2\alpha)\bigg)\bigg]A_\tau(t)\left(\frac{\tau}{T}\right)^2\sin[\omega_1 t - \beta_\tau(t)], \quad (20)$$
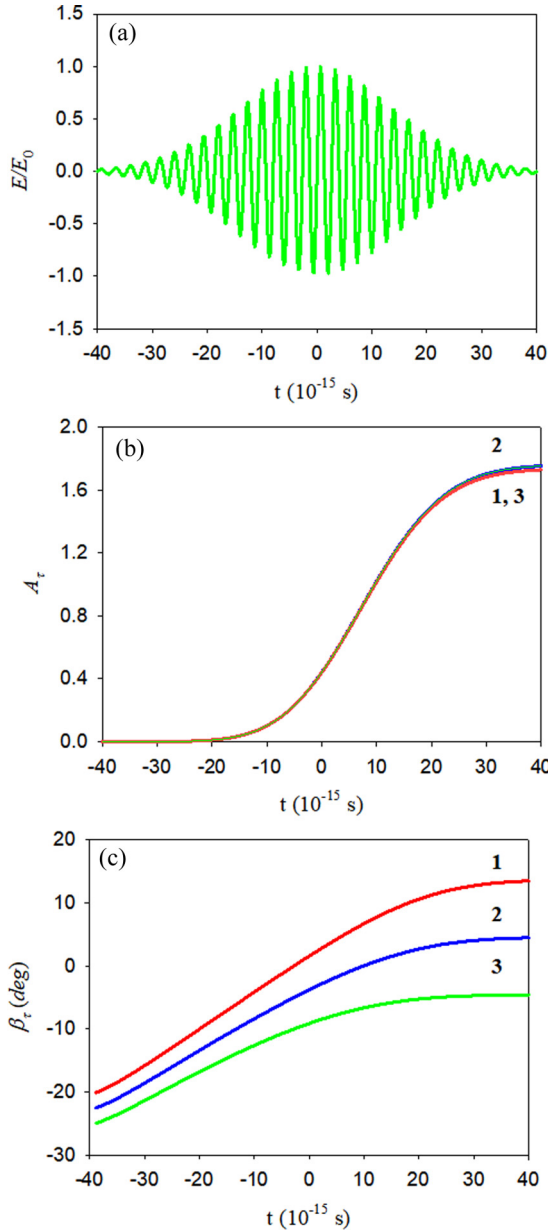
FIG. 1. (a) Shape of the laser pulse, where $E/E_0$ is the normalized electric field of the light pulse; (b) the amplitudes of dynamic magnetization; and (c) the initial magnetization phase $\beta_\tau(t) = \arctan(\text{Im}(F_{\tau-}(t))/\text{Re}(F_{\tau-}(t)))$, where curve 1 stands for $\omega - \omega_0 = -10^{13}$, curve 2 stands for $\omega - \omega_0 = 0$, curve 3 stands for $\omega - \omega_0 = +10^{13}$, and the pulse duration $\tau = 20$ fs.

where $\mu_{\text{eff}} = \mu_B g \sqrt{15\pi}$, $A_\tau(t) = |F_{\tau-}(t)|$ [Fig. 1(b)], $\omega_1 = E_1/\hbar = 10^{13}$ rad/s, $\beta_\tau(t) = \arctan(\text{Im}(F_{\tau-}(t))/\text{Re}(F_{\tau-}(t)))$ [Fig. 1(c)], $c = \mu_B g_J \sqrt{15\pi} (\frac{T}{8\hbar})^2$, $k = 5, 6, 7, 8$ is the number of $Dy^{3+}$ ions in the unit cell (see Fig. 2), and $\pm$ signs in front of the $\boldsymbol{M}^{(k)}$ components correspond to the direction of magnetization of the $k$th ions, i.e., $+$ stands for the fifth and sixth ions, while $-$ stands for the seventh and eighth ions.

Note that while the amplitude $A_\tau(t)$ depends weakly on the frequency difference $\omega - \omega_0$, for the phase $\beta_\tau$ the dependence is significant.
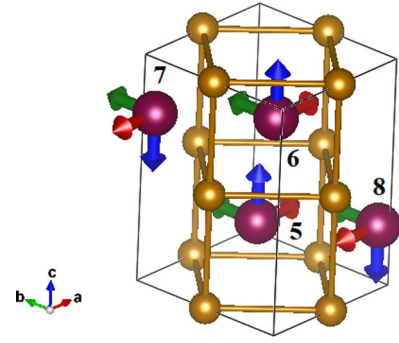


FIG. 2. Unit cell of $DyFeO_3$. Configurations of the components of the magnetic moments of the $Dy^{3+}$ ions induced by a short laser pulse with the central wavelength $\lambda = 0.8$ $\mu$m. Red arrows stand for $M_a^{(k)}$ components, green arrows stand for $M_b^{(k)}$ components, and blue arrows stand for $M_c^{(k)}$ components; $k = 5, 6, 7, 8$. The magnetic moments of the $Dy^{3+}$ ions are oriented parallel to the "$b$" axis and antiparallel to the "$a$" and "$c$" axes, respectively.

Using irreducible representations of the $D_{2h}^{16}$ symmetry group, Eqs. (20) can be represented as

$$C_a = M_a^5 + M_a^6 - M_a^7 - M_a^8$$
$$= \mu_{\text{eff}} E_c E_a (q_1 - q_2) \sin(2\alpha) A_\tau(t) \left(\frac{\tau}{T}\right)^2 \sin[\omega_1 t - \beta_\tau(t)],$$

$$F_b = M_b^5 + M_b^6 + M_b^7 + M_b^8$$
$$= 2\mu_{\text{eff}} E_c E_a (q_1 - q_2) \cos^2 \alpha A_\tau(t) \left(\frac{\tau}{T}\right)^2 \sin[\omega_1 t - \beta_\tau(t)],$$

$$C_c = M_c^5 + M_c^6 - M_c^7 - M_c^8$$
$$= \mu_{\text{eff}} \left[ q_3 E_c^2 + E_a^2 \left( q_3 \sin^2 \alpha + q_4 \cos^2 \alpha \right.\right.$$
$$\left.\left. - \frac{q_1 + q_2}{2} \sin(2\alpha) \right) \right] A_\tau(t) \left(\frac{\tau}{T}\right)^2 \sin[\omega_1 t - \beta_\tau(t)].$$
$$(21)$$

Following the analogy with the spin dynamics of $Fe^{3+}$ ions in $DyFeO_3$, below we will refer to $C_a$ and $C_c$ as antiferromagnetic modes and $F_b$ will be called a ferromagnetic mode. The antiferromagnetic mode $C_a$ and the ferromagnetic mode $F_b$ are transformed according to the irreducible representation $\Gamma_3$. The irreducible representation for the antiferromagnetic mode $C_c$ is $\Gamma_1$. Equations (21) show that the electric field products $E_c E_a$ are coupled with the $C_a$ and $F_b$ modes, while $E_c^2$ and $E_a^2$ excite the $C_c$ mode.

In the case of short pulses at $t > \tau$, one can assume $F_{\tau-}(t) \approx F_{\tau-}(\tau)$. It means that $f_{\tau-}(t) = \exp(-i\omega_1 t) F_{\tau-}(\tau)$, and the dependencies $M_{a,b,c}^{(k)}$ [see (19)] have an oscillating character $M^{(k)} = M_{a(b,c)}^{(k)} \sin(\omega_1 t - \beta_\tau)$, where $\beta_\tau$ is the initial phase determined from the relation $\tan \beta_\tau = \text{Im}(F_{\tau-}(\tau))/\text{Re}(F_{\tau-}(\tau))$ (Fig. 1).

As seen from Eqs. (20), the transient magnetization left after the laser pulse excitation is determined by the dynamic amplitude $A(t)$, the frequency $\omega_1$, and the phase $\beta_\tau(t)$. The properties of the rare-earth ion depend on the CF parameters $q_i$ and on the angle $\alpha$ between the Ising ion axis and the principal crystal axis.

A short pulse of linear polarized light propagating along the $b$-axis induces coherent oscillations of magnetic moments of $Dy^{3+}$ ions in time domain $t > \tau$. The arrangement of magnetic moments can be described as a combination of an "antiferromagnetic part" with magnetic moments in the "$a$-$c$" plane, and a "ferromagnetic part" with magnetic moments aligned along the $b$ axis as shown in Fig. 2.

Note that in the case of monochromatic radiation, the excitation is present for an infinitely long time (see Ref. [12]), and the functions $f_{\tau\pm}$ are real and equal to $f_{\tau\pm} = 2/\sqrt{\pi}\tau^2\omega_1(\omega_0 \pm \omega)$. Hence, in accordance with Eq. (20), monochromatic linearly polarized light, in contrast to pulsed light, does not induce a magnetic textures.

## IV. ULTRAFAST INVERSE QUANTUM FARADAY EFFECT

The electric field $\boldsymbol{E}$ of a circular polarized wave propagating along the "$b$" axis is defined as $\boldsymbol{E} = E_c\boldsymbol{c} + E_a\boldsymbol{a}$, where

$$E_c = E_0 \exp\left(-\frac{t^2}{\tau^2}\right)\cos(\omega t),$$

$$E_a = \pm E_0 \exp\left(-\frac{t^2}{\tau^2}\right)\sin(\omega t), \qquad (22)$$

and then

$$\boldsymbol{E} = \frac{1}{2}E_0 \exp\left[-\left(\frac{t}{\tau}\right)^2\right][\exp(i\omega t)(\boldsymbol{c} \mp i\boldsymbol{a}) + \text{c.c.}]. \quad (23)$$

Here, the upper sign of the $\pm$ notation stays for the left-handed circularly polarized wave, and the lower sign stays for the right-handed circular polarization. Therefore, the operator $\hat{V}_0$ becomes

$$\hat{V}_0 = -\frac{E_0}{2}\sum\gamma_\alpha(k)\hat{D}_{\text{eff}\alpha}, \qquad (24)$$

where $\gamma_\alpha(k) = (\boldsymbol{c} \mp i\boldsymbol{a})e_k^\alpha$.

Taking for circularly polarized light

$$E_\alpha(k) = \frac{E_0}{2}\gamma_\alpha(k) \qquad (25)$$

using Eqs. (C1) from Appendix C and, similarly to the treatment explained in Sec. II, limiting ourselves to the main terms in (C1) for nearly resonant conditions $\omega \approx \omega_0$, we find

$$M_a^{(k)} = \pm(-1)^m\mu_{\text{eff}}E_0^2\left(q_3\sin^2\alpha + \frac{q_1+q_2}{4}\sin(2\alpha)\right),$$

$$\times A_\tau(t)\left(\frac{\tau}{T}\right)^2\cos[\omega_1 t - \beta_\tau(t)],$$

$$M_b^{(k)} = (-1)^m\mu_{\text{eff}}E_0^2\left(q_3\frac{\sin^2(\alpha)}{2} + \frac{q_1+q_2}{2}\cos^2\alpha\right),$$

$$\times A_\tau(t)\left(\frac{\tau}{T}\right)^2\cos[\omega_1 t - \beta_\tau(t)],$$

$$M_c^{(k)} = \mp\mu_{\text{eff}}E_0^2\left(q_3(1 + \sin^2\alpha) + q_4\cos^2\alpha\right.$$

$$\left. -\frac{q_1+q_2}{2}\sin(2\alpha)\right)A_\tau(t)\left(\frac{\tau}{T}\right)^2\cos[\omega_1 t - \beta_\tau(t)],$$

$$\qquad (26)$$

where $m = 1$ if light is left-handed circularly polarized, and $m = 2$ if light is right-handed circularly polarized.

Rewriting Eqs. (26) in terms of irreducible representations of the $D_{2h}^{16}$ symmetry group, one obtains

$$C_a = M_a^5 + M_a^6 - M_a^7 - M_a^8,$$

$$= (-1)^m\mu_{\text{eff}}E_0^2\left(q_3\sin^2\alpha + \frac{q_1+q_2}{4}\sin(2\alpha)\right)$$

$$\times A_\tau(t)\left(\frac{\tau}{T}\right)^2\cos[\omega_1 t - \beta_\tau(t)],$$

$$F_b = M_b^5 + M_b^6 + M_b^7 + M_b^8$$

$$= (-1)^m\mu_{\text{eff}}E_0^2\left(q_3\frac{\sin^2(\alpha)}{2} + \frac{q_1+q_2}{2}\cos^2\alpha\right)$$

$$\times A_\tau(t)\left(\frac{\tau}{T}\right)^2\cos[\omega_1 t - \beta_\tau(t)],$$

$$C_c = M_c^5 + M_c^6 - M_c^7 - M_c^8$$

$$= \mu_{\text{eff}}E_0^2\left(q_3(1 + \sin^2\alpha) + q_4\cos^2\alpha\right.$$

$$\left. -\frac{q_1+q_2}{2}\sin(2\alpha)\right)A_\tau(t)\left(\frac{\tau}{T}\right)^2\cos[\omega_1 t - \beta_\tau(t)].$$

$$\qquad (27)$$

In the case $t > T$, the $M_{a,b,c}^{(k)}$ components induced by the wave field have an oscillating character that is proportional to $\cos(\omega_1 t - \beta_\tau)$. Note that $M_c$ are independent of the helicity of circularly polarized light [see Eq. (26)] and the dependencies of magnetization amplitudes on the orientation of the Ising axis are different in the cases of linearly polarized and circularly polarized pulses [see Eqs. (20) and (26)].

Let us explore using Eqs. (20) and (26) the influence of pulse duration on the amplitudes and phases of oscillations corresponding to the magnetic modes. We consider ultrashort light pulses of the same fluence, and we write the electric field of the interacting light wave in the form

$$E(\tau, t) = E_0(\tau)\exp(-t^2/\tau^2)\sin(\omega t), \qquad (28)$$

where $\omega = 2\pi/T$, and $T$ is the wave period (for $\lambda = 0.8\ \mu$m, $T = 8/3$ fs). It can be shown that

$$E_0^2(\tau)\int_{-\infty}^{\infty}[\exp(-t^2/\tau^2)\sin(\omega t)]dt$$

$$= E_0^2(\tau)\tau\sqrt{\frac{\pi}{8}}\left\{1 - \exp\left[-2\left(\frac{\pi\tau}{T}\right)^2\right]\right\} = \text{const.} \quad (29)$$

At $\tau \geqslant T$, one gets $\exp[-2(\frac{\pi\tau}{T})^2] \ll 1$, and in this case Eq. (29) is equivalent to the relation $E_0^2(\tau)\tau = \text{const}$. It is easy to see that the oscillations of magnetic modes excited by light pulses under the condition $E_0(\tau) \approx 1/\sqrt{\tau}$ can be represented in the form

$$\mu_{\alpha i} = M(\mu, \alpha, i)m_i(\tau, t), \qquad (30)$$

where the symbol $\mu$ determines the modes $C$ and $F$, $\alpha$ are the axes $a, b, c$, and the index $i = 1, 2$ indicates whether we discuss the cases of a linearly polarized pump or the inverse Cotton effect ($i = 1$), or a circularly polarized pump and
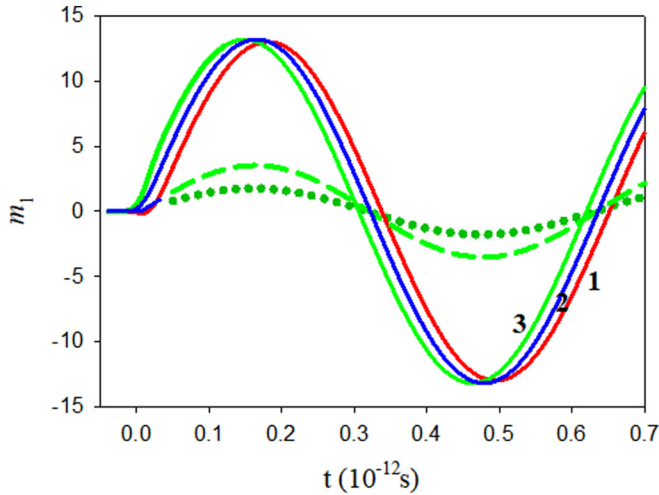
FIG. 3. Magnetization dynamics of $Dy^{3+}$ ions triggered by linearly polarized laser pulse. The dependencies $m_1(t)$ are determined by Eq. (31). The effect of light on the ion magnetization can be seen as the inverse Cotton-Mouton effect [32,33]. Red curve 1 stands for $\omega - \omega_0 = -10^{13}$, blue curve 2 stands for $\omega - \omega_0 = 0$, green curve 3 stands for $\omega - \omega_0 = +10^{13}$, the pulse duration $\tau = 20$ fs, the dashed curve corresponds to $\tau = 2T$, and the dotted curve corresponds to $\tau = T$.

FIG. 4. Magnetization dynamics of $Dy^{3+}$ ions induced by circularly polarized light. The dependencies $m_2(t)$ are determined by Eq. (31). The effect can be seen as the ultrafast inverse Faraday effect. Red curve 1 stands for $\omega - \omega_0 = -10^{13}$, blue curve 2 stands for $\omega - \omega_0 = 0$, green curve 3 stands for $\omega - \omega_0 = +10^{13}$, the pulse duration $\tau = 20$ fs, the dashed curve corresponds to $\tau = 2T$, and the dotted curve corresponds to $\tau = T$.

the inverse Faraday ($i = 2$) effect, respectively. The dimensionless function $m_i(\tau, t)$ describing the dynamics of modes has the form

$$m_i(\tau, t) = A_\tau(t)\frac{\tau}{T} \sin\left(\omega_1 t - \beta_\tau(t) + \frac{\pi}{2}(i - 1)\right). \quad (31)$$

In Eq. (30), $M(\mu, \alpha, i)$ are the quantities that do not depend on $t$ and $\tau$, the form of which for each specific mode and effect can be easily found from a comparison of Eqs. (20), (26), and (30).

Dependencies of $m_i$ on $t$ for different $\tau$ are shown in Figs. 3 and 4. A significant decrease in the amplitudes of the steady-state oscillations of magnetic modes (at $t > \tau$) upon a decrease in the pulse duration is clearly seen from the figures.

Hence, we have shown that after excitation with a short laser pulse, transient magnetization dynamics of $Dy^{3+}$ ions depends on both the properties of the ions and detuning between the central frequency of the laser excitation and the resonant frequencies of the electronic transition in $Dy^{3+}$. The amplitude and the phase of the stabilized oscillations, as well as the process of establishing these values in time, depend on the shape and duration of the pulse. We also highlight the difference in magnetization dynamics triggered by linearly and circularly polarized pulses. Polarized laser pulses excite oscillating magnetic moments of $Dy^{3+}$ resembling antiferromagnetic and ferromagnetic modes of $Fe^{3+}$ spin resonances. In the same way, the influence of circularly and linearly polarized light on the magnetic moment $Dy^{3+}$ can be considered as the inverse Faraday and Cotton-Mouton effects, respectively. Note that the oscillations of the magnetic moments in the inverse Faraday and Cotton-Mouton effects are phase-shifted by $\pi/2$.
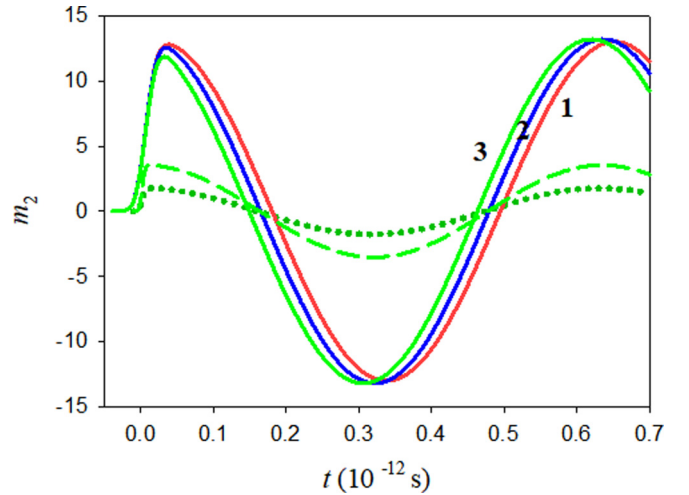
## V. CONCLUSION

Upgrading the theoretical framework for the inverse magneto-optical effects suggested by Pershan *et al.* [28] and making it applicable to the case of femtosecond laser pulses, we explored the laser-induced magnetization dynamics in $Dy^{3+}$ ions.

Our findings show that ultrashort laser pulses excite new dynamic textures of magnetic moments of $Dy^{3+}$ ions in $DyFeO_3$. These textures resemble ferromagnetic and antiferromagnetic modes of magnetic resonance in $DyFeO_3$. After laser excitation, the magnetic moments coherently oscillate at the frequency of the electronic transition from the ground to the low-lying state in the $Dy^{3+}$ ion. The damping of magnetic oscillations is determined by the relaxation time of the rare-earth ions, which is about 10 ps.

On the timescales of the pulse duration, the entire dynamics of magnetization, including the phase of oscillations, can be tuned using the form factor calculated in this work. The transient magnetic textures predicted in this work can be investigated using advanced ultrafast imaging techniques and advanced sources of light such as free-electron lasers [34,35]. We believe that our theoretical result may be of interest for further experiments aiming to understand the magnetization dynamics of rare-earth ions.

Finally, we note that here we neglected the effects induced by the $Fe^{3+}$ sublattices. In orthoferrites, the frequencies of the ferromagnetic and antiferromagnetic resonances for $Fe^{3+}$ ions are rather far from the frequencies of the magnetization dynamics of $Dy^{3+}$ ions.

## APPENDIX A: ELECTRIC-DIPOLE INTERACTIONS IN RARE-EARTH IONS AND THE TRANSITION $^6H_{15/2} \rightarrow {}^6F_{5/2}$ IN DyFeO$_3$

The Hamiltonian of a crystal field acting on the rare-earth ions in orthoferrite contains odd terms since the point symmetry group $C_s$ of their environment lacks a space inversion element [the reflection in the "$a$-$b$" plane ($C_s$) corresponds to the change $x \rightarrow -x$]. In the general case, the crystal field Hamiltonian reads

$$\hat{V}_{cr} = \sum r^t b^t_\tau \hat{c}^t_\tau, \tag{A1}$$

where $\hat{c}^t_\tau$ are the one-electron irreducible operators of the order "$t$," and $b^t_\tau$ are the crystal-field parameters. The fifth and seventh terms in (A1) representing the allowance of the transition $^6H_{15/2} \rightarrow {}^6F_{5/2}$ read

$$\begin{aligned} V_{odd} &= r^5 b^5_0 \hat{c}^5_0 + r^5 b^5_1 i(\hat{c}^5_1 + \hat{c}^5_{-1}) + r^5 b^5_2(\hat{c}^5_2 + \hat{c}^5_{-2}) \\ &\quad + r^5 b^5_3 i(\hat{c}^5_3 + \hat{c}^5_{-3}) + r^5 b^5_4(\hat{c}^5_4 + \hat{c}^5_{-4}) \\ &\quad + r^5 b^5_5 i(\hat{c}^5_5 + \hat{c}^5_{-5}). \end{aligned} \tag{A2}$$

We restrict ourselves by reducing of the fifth-order terms in (A2). Interaction of a rare-earth ion with the electric field $\boldsymbol{E}$ reads

$$\hat{V}_E = -\boldsymbol{E}\boldsymbol{d} = e\boldsymbol{E} \sum_n r_n. \tag{A3}$$

Interactions (A2) and (A3) mix states of the ground configuration $l^N$ ($l = 3$ is the orbital quantum number of the $4f$ shell) and $l^N l'$ ($l' = l \pm 1$) configurations of excited states, displaced from the ground state in energy on $W_{l'} = 10^5$ cm$^{-1}$. We project $V = V_{odd} + V_E$ on the space of functions of the ground configuration $4f^N$, and we obtain the matrix $(V_{eff})_{12} = -\sum \frac{V_{1k}V_{k2}}{W_k}$, where states $|1\rangle$ and $|2\rangle$ belong to the $4f^N$ configuration, and $|k\rangle$ are the states of $l^N l'$ configurations. Terms of matrix $(V_{eff})_{12}$ linear in $\boldsymbol{E}$ components can be represented by the effective Hamiltonian (for details, see [30])

$$\begin{aligned} \hat{H}_{me} &= 2 \sum_{\mu t \tau l'} \sum_{nm} (-1)^\mu E_{-\mu} B^t_\tau(ll') A(ll'tn) W^{-1}_{l'} \\ &\quad \times C^{nm}_{1\mu t\tau} \hat{c}^{\hat{n}}_m, \end{aligned} \tag{A4}$$

where $t$ and $\tau$ corresponds to ones given in eq. (A2), $\mu = 0, \pm 1$; $n = 2, 4, 6$; $m = -n \div n$; $l' = l \pm 1$,

$$E_{+1} = -\frac{1}{\sqrt{2}}(E_x + iE_y),$$

$$E_{-1} = \frac{1}{\sqrt{2}}(E_x - iE_y),$$

$$E_0 = E_z,$$

are the circular components of vector $E_\mu$,

$$A(ll', tn) = -er_{ll'} \frac{C^{l0}_{l'010} C^{l'0}_{l0r0}}{C^{l0}_{l0n0}} \begin{pmatrix} t1n \\ lll \end{pmatrix} \sqrt{(2l'+1)(2l+1)},$$

and $C^{nm}_{1\mu t\tau}$ and $\begin{pmatrix} abc \\ def \end{pmatrix}$ are the Clebsh-Gordon coefficients and the $6j$ symbols, respectively.

To obtain Eq. (A4), we neglected the splitting of $4f^{N-1}5d$ ($l' = 2$) and $4f^{N-1}5g$ ($l' = 4$) configurations. Expression (A4) is valid for odd crystal fields of a general form. Specifically for (A2), taking into account only the $4f^{N-1}5d$ configuration, we get $H^{(5)}_{me} = -\sum_\alpha E_\alpha D_{eff\alpha}$,

$$\begin{aligned} D_{eff,x} &= A \left[ B^5_3 \sqrt{\frac{15}{14}} i(C^6_{-4} - C^6_4) + B^5_4 \sqrt{\frac{15}{12}}(C^6_{-5} - C^6_5) \right. \\ &\quad \left. + \frac{B^5_3}{\sqrt{2}} i(C^6_{-6} - C^6_6) \right], \end{aligned}$$

$$\begin{aligned} D_{eff,y} &= A \left[ -B^5_3 \sqrt{\frac{15}{14}}(C^6_{-4} + C^6_4) + iB^5_4 \sqrt{\frac{15}{12}}(C^6_{-5} + C^6_5) \right. \\ &\quad \left. - \frac{B^5_3}{\sqrt{2}}(C^6_{-6} + C^6_6) \right], \end{aligned}$$

$$D_{eff,z} = A \left[ B^5_4 \sqrt{\frac{10}{33}}(C^6_{-4} + C^6_4) + B^5_3 i(C^6_{-5} + C^6_5) \right], \tag{A5}$$

where $A = \frac{P_0}{W_d} \sqrt{\frac{6 \times 13}{7 \times 11}}$ and $B^5_q = r^5_{fd} b^5_q$ are the parameters of the odd CF. In (A5) we keep only actual terms containing operators $C^6_m$, $m = \pm 4, \pm 5, \pm 6$. In the general case, operators of the effective dipole moment $D_{eff\alpha}$ are of the form (13); in this case, $V_{odd}$ accounts the seventh-order terms and $4f^{N-1}5g$ configurations.

## APPENDIX B: EFFECTIVE DIPOLE MOMENTS $D_{eff}$ OF THE RARE-EARTH IONS IN DyFeO$_3$

DyFeO$_3$ is an antiferromagnet, where antiferromagnetically coupled Fe$^{3+}$ ions are also exchange coupled to paramagnetic Dy$^{3+}$ ions. Exchange interaction between Fe$^{3+}$ and Dy$^{3+}$ ions results in an effective magnetic field that acts on Dy$^{3+}$ ion. The magnetic structures of DyFeO$_3$ and its evolution as a function of temperature were explored in Refs. [23,36], where it was shown that depending on temperature, the structure transforms according to the $\Gamma_1$ and $\Gamma_4$ representations.

In the phase $\Gamma_1$ below the Morin temperature $T_M = 40$ K, the effective magnetic field from the exchange interaction between Dy$^{3+}$ and Fe$^{3+}$ ions is equal to zero. In the phase $\Gamma_4$ at higher temperatures $T > T_M$ a nonzero magnetic field along the $c$ axis (local "$x$" axis) mixes the $|\pm 15/2\rangle$ and the $|\pm 13/2\rangle$ doublets without splitting.

At $E = 0$ the wave functions of an ion ground state read

$$|\pm g_0\rangle = |\pm 15/2\rangle - h_x|\pm 13/2\rangle,$$

$$|\pm f\rangle = |\pm 13/2\rangle - h_x|\pm 15/2\rangle, \tag{B1}$$

where $h_x = \sqrt{15} g_J \mu_B H_x / 2\omega_1 \hbar \approx 0.1$, $\boldsymbol{H}$ is the effective magnetic field acting on the Dy$^{3+}$ at $T > T_M$, at $T < T_M$ $H = 0$, and $\omega_1 \hbar = E_1 \approx 52$ cm$^{-1}$.

The actual components of $\hat{D}_{eff}$ for the transition determined in the local axes [see (C1) and Appendix A]

$$\begin{aligned} D_{eff,x} &= K_4 i(C^6_{-4} - C^6_4) + K_5(C^6_{-5} - C^6_5) \\ &\quad + K_6 i(C^6_{-6} - C^6_6), \end{aligned}$$

$$D_{\text{eff},y} = -K_4\big(C_{-4}^6 + C_4^6\big) + K_5 i\big(C_{-5}^6 + C_5^6\big)$$
$$- K_6\big(C_{-6}^6 + C_6^6\big),$$
$$D_{\text{eff},z} = -K_4'\big(C_{-4}^6 + C_4^6\big) + K_5' i\big(C_{-5}^6 + C_5^6\big)$$
$$- K_6'\big(C_{-6}^6 + C_6^6\big), \tag{B2}$$

where $C_{\pm m}^6$ are the actual irreducible tensor operators of the crystal field, and $K_m$ and $K_m'$ are the magnitudes that are dependent on the odd CF parameters, which are of the form (see Appendix A) $K \approx P_0 B_q^5/W_d$, where $P_0 = er_{fd}$ is the elementary dipole moment of $Dy^{3+}$, $r_{fd} \approx 0.04$ nm is the radial integral [37], and $W_d \approx 10^5$ cm$^{-1}$ is the difference between the energies of the $4f^{N-1}5d$ and $4f^N$ configurations [31]. The CF parameters $B_q^k$ can attain values of the order of $10^3$ cm$^{-1}$ according to [38] for $Pr^{3+}$ in $PrFe_3(BO_3)_4$, $B_3^5 = 2170$ cm$^{-1}$. Thus, $K \approx P_0\xi$, $\xi \approx 10^{-2}$.

### APPENDIX C: WAVE FUNCTIONS OF THE Dy$^{3+}$ION IN DyFeO$_3$

The ground state of the $Dy^{3+}$ ion is the $^6H_{15/2}$ Ising doublet. It is described by $|\pm 15/2\rangle$ wave functions determined in the local reference frame, where the $z$-axis lies in the "$a$-$b$" plane at the angles $\alpha = \pm 60°$ to the axis "$a$" [38]. The local symmetry axes of four $Dy^{3+}$ ions in the DyFeO$_3$ unit cell are determined as follows:

$$\boldsymbol{e}_k^x = (0, 0, (-1)^k), \; \boldsymbol{e}_{1,2}^y = (-\sin(\alpha), \pm\cos(\alpha), 0),$$
$$\boldsymbol{e}_k^x = (\cos(\alpha), \pm\sin(\alpha), 0), \; \boldsymbol{e}_{3(4)}^y = -\boldsymbol{e}_{1(2)}^y,$$
$$\boldsymbol{e}_{3(4)}^z = -\boldsymbol{e}_{1(2)}^z. \tag{C1}$$

CF splits multiplet $^6H_{15/2}$ into two doublets with the energies $E_0 = 0$, $E_1 \approx 52$ cm$^{-1}$, $E_2 \approx 147$ cm$^{-1}$, $E_3 \approx 225$ cm$^{-1}, \ldots$, etc. [21]. The first excited doublets are the Ising doublets described by the wave functions $|\pm 13/2\rangle$ in the local reference frame (C1).

We neglect splitting of multiplet $^6F_{5/2}$ in the CF and exchange field. The unperturbed wave functions of the ground state $\phi_g$ and $\phi_f$ are determined by Eq. (B1), and for a laser pulse with a central photon energy of 1.5 eV, the wave functions of an intermediate state $^6F_{5/2}$ are determined by $\phi_m = |m\rangle$, where $m = \pm 1/2, \pm 3/2, \pm 5/2$ is the magnetic quantum number of the $^6F_{5/2}$ ($J' = 5/2$) states.

Let us obtain the actual expressions for $a_{fg}^{(2)}(t)$ and $\psi_{2g}(t)$ functions for Gaussian laser pulse induced excitations of the $Dy^{3+}$ ion in orthoferrites and orthoaluminates.

Substituting the expressions for $\phi_g, \phi_f, \phi_l \to |m\rangle$ as well as the pulse shape $v(t)$ in Eq. (7) and integrating them over $t''$ yields

$$a_{\pm f\pm g}^{(2)} = -\frac{\sqrt{\pi}}{2}\frac{\tau^2}{\hbar^2}\sum_m [\langle\pm f|v_0^*|m \times m|v_0| \pm g\rangle F_{\tau+}(t)$$
$$+ \langle\pm f|v_0|m \times m|v_0^*| \pm g\rangle F_{\tau-}(t)], \tag{C2}$$

where

$$F_{\tau\pm}(t) = \frac{1}{\tau}\int_{-\infty}^t \phi_\pm(t')dt', \tag{C3}$$

$$\phi_{(\pm)}(t) = \exp\left(-\frac{2t^2}{\tau^2} + i\omega_1 t\right)\exp[Z_\pm^2(t)]\text{erfc}[Z_\pm(t)], \tag{C4}$$

$$Z_\pm(t) = \frac{i}{2}\tau(\omega_0 \pm \omega) - \frac{t}{\tau}. \tag{C5}$$

In Eq. (C5), $\omega_0 = (E_J' - E_0)/\hbar \approx 12 \times 10^3$ cm$^{-1}$, and $E_J'$ is the weighted median energy of multiplet $^6F_{5/2}$. In Eq. (C2) we neglected the terms comprising $\exp(\pm 2i\omega t)$ in accordance with the rotating-wave approximation.

Consider the wave functions $\psi_g(t) = \phi_g + \psi_{2g}(t)$ [see (3), (5), (B1), and (C2)] and represent them in the zero in $h$ approximation,

$$|\pm g\rangle = |\pm 15/2\rangle + Q_\pm^{(2)}(E, t)|\pm 13/2\rangle, \tag{C6}$$

$$Q_\pm^{(2)}(E, t) = \sqrt{\pi}[q_\pm^{(2)}(E^*E)f_{\tau+}(t)$$
$$+ q_\pm^{(2)}(EE^*)f_{\tau-}(t)], \tag{C7}$$

$$q_\pm^{(2)}(EE^*) = \pm(q_1 E_\mp E_z^* - q_2 E_z E_\pm^*) - i(q_3 E_\mp E_\pm^* + q_4|E_z|^2),$$
$$E_\pm = E_x \pm iE_y,$$
$$E_\pm^* = E_x^* \pm iE_y^*, \tag{C8}$$

$$q_1 = \left(\frac{T}{8\hbar}\right)^2 R\big(C_{5/25/264}^{15/2\,13/2}C_{5/25/265}^{15/2\,15/2}K_4K_5'$$
$$- K_5K_6'C_{5/23/265}^{15/2\,13/2}C_{5/23/266}^{15/2\,15/2}\big),$$
$$q_2 = q_1(K \rightleftharpoons K'),$$
$$q_3 = q_1(K' \to K),$$
$$q_4 = q_1(K \to K'), \tag{C9}$$

where $R = \langle^6F_{5/2}\|C^6\|^6H_{15/2}\rangle$ is the reduced matrix element, $R = 10^0$–$10^{-1}$, and $C_{a\alpha b\beta_\tau}^{c\gamma}$ are the Clebsh-Gordon coefficients: $C_{5/25/264}^{15/2\,13/2} = \sqrt{\frac{2\times 11}{13\times 17}}$, $C_{5/25/265}^{15/2\,15/2} = \sqrt{\frac{5}{17}}$, $C_{5/23/265}^{15/2\,13/2} = -\frac{7}{\sqrt{15\times 17}}$, $C_{5/23/266}^{15/2\,15/2} = -\sqrt{\frac{12}{17}}$,

$$f_{\tau\pm} = \exp(-i\omega_1 t)F_{\tau\pm}(t). \tag{C10}$$

[1] E. Beaurepaire, J.-C. Merle, A. Daunois, and J.-Y. Bigot, Phys. Rev. Lett. **76**, 4250 (1996).

[2] F. Siegrist, J. A. Gessner, M. Ossiander, C. Denker, Y.-P. Chang, M. C. Schröder, A. Guggenmos, Y. Cui, J.

Walowski, U. Martens *et al.*, Nature (London) **571**, 240 (2019).

[3] J. K. Dewhurst, P. Elliott, S. Shallcross, E. K. Gross, and S. Sharma, Nano Lett. **18**, 1842 (2018).

[4] P. Němec, M. Fiebig, T. Kampfrath, and A. V. Kimel, Nat. Phys. **14**, 229 (2018).

[5] A. J. Schellekens and B. Koopmans, Phys. Rev. B **87**, 020407(R) (2013).

[6] F. Willems, C. von Korff Schmising, C. Strüber, D. Schick, D. W. Engel, J. K. Dewhurst, P. Elliott, S. Sharma, and S. Eisebitt, Nat. Commun. **11**, 871 (2020).

[7] A. V. Kimel, A. Kirilyuk, P. Usachev, R. Pisarev, A. Balbashov, and T. Rasing, Nature (London) **435**, 655 (2005).

[8] A. V. Kimel, A. Kirilyuk, F. Hansteen, R. V. Pisarev, and T. Rasing, J. Phys.: Condens. Matter **19**, 043201 (2007).

[9] J. Tang, Y. Ke, W. He, X. Zhang, W. Zhang, N. Li, Y. Zhang, Y. Li, and Z. Cheng, Adv. Mater. **30**, 1706439 (2018).

[10] K. Grishunin, T. Huisman, G. Li, E. Mishina, T. Rasing, A. V. Kimel, K. Zhang, Z. Jin, S. Cao, W. Ren *et al.*, ACS Photon. **5**, 1375 (2018).

[11] B. Ivanov, Low Temp. Phys. **40**, 91 (2014).

[12] S. Baierl, M. Hohenleutner, T. Kampfrath, A. Zvezdin, A. Kimel, R. Huber, and R. Mikhaylovskiy, Nat. Photon. **10**, 715 (2016).

[13] J. De Jong, A. Kalashnikova, R. Pisarev, A. Balbashov, A. Kimel, A. Kirilyuk, and T. Rasing, J. Phys.: Condens. Matter **29**, 164004 (2017).

[14] D. Afanasiev, B. A. Ivanov, A. Kirilyuk, T. Rasing, R. V. Pisarev, and A. V. Kimel, Phys. Rev. Lett. **116**, 097401 (2016).

[15] R. Mikhaylovskiy, E. Hendry, A. Secchi, J. H. Mentink, M. Eckstein, A. Wu, R. Pisarev, V. Kruglyak, M. Katsnelson, T. Rasing *et al.*, Nat. Commun. **6**, 8190 (2015).

[16] C. D. Stanciu, F. Hansteen, A. V. Kimel, A. Kirilyuk, A. Tsukamoto, A. Itoh, and T. Rasing, Phys. Rev. Lett. **99**, 047601 (2007).

[17] A. V. Kimel, A. Kirilyuk, A. Tsvetkov, R. Pisarev, and T. Rasing, Nature (London) **429**, 850 (2004).

[18] M. Deb, P. Molho, B. Barbara, and J.-Y. Bigot, Phys. Rev. B **97**, 134419 (2018).

[19] R. V. Mikhaylovskiy, T. J. Huisman, A. I. Popov, A. K. Zvezdin, T. Rasing, R. V. Pisarev, and A. V. Kimel, Phys. Rev. B **92**, 094437 (2015).

[20] R. Iida, T. Satoh, T. Shimura, K. Kuroda, B. A. Ivanov, Y. Tokunaga, and Y. Tokura, Phys. Rev. B **84**, 064402 (2011).

[21] H. Schuchert, S. Hüfner, and R. Faulhaber, Z. Phys. A **220**, 273 (1969).

[22] G. Gorodetsky, B. Sharon, and S. Shtrikman, Solid State Commun. **5**, 739 (1967).

[23] K. Belov, A. Zvezdin, A. Kadomtseva, and R. Levitin, *Spin-reorientation Transitions in Rare Earth Magnets* (Nauka, Moscow, 1979).

[24] D. Popova, A. Bringer, and S. Blügel, Phys. Rev. B **85**, 094419 (2012).

[25] D. Popova, A. Bringer, and S. Blügel, Phys. Rev. B **84**, 214421 (2011).

[26] J. D. Axe Jr., J. Chem. Phys. **39**, 1154 (1963).

[27] S. Washimiya, J. Phys. Soc. Jpn. **27**, 56 (1969).

[28] P. Pershan, Phys. Rev. **143**, 574 (1966).

[29] J. Van der Ziel, P. Pershan, and L. Malmstrom, Phys. Rev. Lett. **15**, 190 (1965).

[30] A. I. Popov, D. I. Plokhov, and A. K. Zvezdin, Phys. Rev. B **87**, 024413 (2013).

[31] K. N. R. Taylor and M. I. Darby, *Physics of Rare Earth Solids* (Springer Science+Business Media, New York, 1972).

[32] B. A. Zon, V. Y. Kupershmidt, G. V. Pakhomov, T. T. Urazbaev, Sov. Phys. Lett. **45**, 272 (1987).

[33] A. M. Kalashnikova, A. V. Kimel, R. V. Pisarev, V. N. Gridnev, A. Kirilyuk, and T. Rasing, Phys. Rev. Lett. **99**, 167205 (2007).

[34] H. N. Chapman, A. Barty, M. J. Bogan, S. Boutet, M. Frank, S. P. Hau-Riege, S. Marchesini, B. W. Woods, S. Bajt, W. H. Benner *et al.*, Nat. Phys. **2**, 839 (2006).

[35] M. Malvestuto, R. Ciprian, A. Caretta, B. Casarin, and F. Parmigiani, J. Phys.: Condens. Matter **30**, 053002 (2018).

[36] A. Zvezdin, V. Matveev, A. Mukhin, and A. Popov, *Rare-earth Ions in Magnetically Ordered Crystals* (Nauka, Moscow, 1985) (in Russian).

[37] B. Judd, Phys. Rev. **127**, 750 (1962).

[38] M. N. Popova, T. N. Stanislavchuk, B. Z. Malkin, and L. N. Bezmaternykh, Phys. Rev. B **80**, 195101 (2009).